An efficient multiple time-scale reversible integrator for the gravitational N-body problem

Ben Leimkuhler *,1

Abstract

A large gravitational (or classical atomic) N-body simulation typically includes fast binary stars, planet-moon systems, or other tightly bound objects, demanding a small timestep and effectively limiting the time interval over which simulation can take place. While ad-hoc averaging schemes have been used before, these are generally neither symplectic nor reversible, impairing their long time-interval stability properties. In this article, we describe the design of a powerful reversible integrator based on partitioning, averaging, reversible adaptive timestepping, and smooth force decomposition. This method also incorporates a modification of the reversible averaging method of [8] based on an interpolation of the forces acting on the fast variables which is potentially much more efficient than the original method.

Key words: N-body problems, Hamiltonian systems, time-reversible discretization, averaging.

1 Introduction

Gravitational N-body problems were some of the first applications of numerical analysis, with a substantial amount and variety of work on the topic appearing long before the advent of the modern computer. In the first half of the last century, in particular, research on the numerical solution of differential equations by Brouwer, Cowell, Kutta, Milne, Moulton, Runge, Störmer, and others was largely motivated by the demands of astronomers for accurate orbits for the planets, the moon and

* Multidisciplinary Modelling Centre, Mathematics Building, University of Leicester, LE1 7RH, UK, Email: bl12@mcs.le.ac.uk

[1] Research supported by the UK Engineering and Physical Sciences Research Council under Grant No. EPSRC GR/R03259.

comets. It is a testament to the depth and importance of this topic that the design of numerical methods for gravitational N-body problems remains an active area of research, with a great deal of study being conducted to understand the formation, structure and long-term evolution of planetary and stellar systems [1–5].

When a gravitational N-body system includes fast oscillatory components due to tightly bound pairs of bodies (or *binaries*), an efficient numerical procedure for simulating the dynamics of the system must treat the fast components differently from the other variables. One option is to collapse a binary to a mass point, an approximation which is adequate for many purposes. On the other hand, the presence of slowly evolving (or even fixed) distant bodies will lead to changes in the orbit of the binary, potentially eventually destabilizing the pair in question or affecting its interactions with other fast components in the system. While formulae for the fluctuation in eccentricity can be developed, these approximations cannot fully account for all the possible complex interactions in a large multi-body system.

As an alternative to standard numerical methods, it is natural to seek some sort of multirate [9] or multiple timestepping [10,11] scheme. In multirate (sometimes *individual timestep* [6]) methods, fast variables are propagated with smaller stepsize. In multiple timestepping, popular in molecular dynamics, the potential energy is decomposed into strong and weak terms, and all bodies in the system are evolved using only the strongest forces and a small timestep, with occasional kicks due to the weaker forces. This is closely related to the *mapping method* of Wisdom and Holman [12]. Unfortunately, both multirate and multiple timestep methods lead to *stepsize resonances*, in practice severely limiting the size of a timestep in proportion to the shortest wavelength.

Averaging techniques [13] have been found to substantially improve the situation, although in molecular dynamics, the increase in the stable timestep is only a factor of about two at most [14]. A new class of averaged methods was suggested in [8]. This method relies on a decomposition of the variables of the system into fast and slow components (as in multirate methods), an accurate fast integration, and a carefully chosen averaging of the forces acting on the slow variables. These methods do not exhibit resonances, at least for certain choices of the averaging interval, and have enabled stable long-term integrations at large timesteps.

One of the positive features of multiple timestepping is that it can be done in a symplectic framework, that is, preserving the two form $\sum_i dq_i \wedge dp_i$ with respect to positions $q_1, \ldots, q_{3N}$ and canonically conjugate momenta $p_1, \ldots, p_{3N}$. Numerous recent studies have demonstrated the significance of this conservation property for the stability of a numerical simulation. Reversible methods, too, have been found to be effective in practice, although there are still gaps in the understanding of these methods at present. It is known, for example, that reversible methods exhibit linear error growth when applied to integrable systems [15].

The idea of the method described herein is to combine the advantages of a reversible integrator for the slow variables with a stable treatment of the tightly coupled fast dynamics, using appropriate timesteps and methods for each problem. The particular challenges associated with gravitational dynamics include (1) the need for adaptive stepsizes, and (2) the need for regularization in close approaches. We argue here that various techniques such as reversible variable stepsizes and regularization can (and must) be combined with the reversible averaging method to generate stable long-term simulations with potentially dramatic benefits in efficiency.

2 The Reversible Averaging Method

We briefly summarize the reversible averaging method; more details may be found in [8]. Consider a conservative system with Hamiltonian

$$H(q,p,\theta,\pi) = \frac{1}{2}p^T M^{-1} p + \frac{1}{2}\pi^T \hat{M}^{-1}\pi + V(q,\theta). \tag{1}$$

Observe that the differential equations on this Hamiltonian are

$$\frac{d}{dt}q = M^{-1}p, \tag{2}$$
$$\frac{d}{dt}\theta = \hat{M}^{-1}\pi, \tag{3}$$
$$\frac{d}{dt}p = -\nabla_q V(q,\theta), \tag{4}$$
$$\frac{d}{dt}\pi = -\nabla_\theta V(q,\theta). \tag{5}$$

While there are several approaches to the derivation of symplectic integrators, the best methods are generally constructed from a *splitting* of the Hamiltonian. Another, related, class of schemes can be constructed by a symmetric concatenation of flows on components of the vector field itself.

Denote the entire vector of phase variables by z and the vector field, i.e. the right hand side of (2)–(5), by $F = F(z)$. Now introduce a splitting of the vector field F as follows:

$$F(z) = F_1 + F_2,$$

where

$$F_1 = \begin{bmatrix} 0 \\ 0 \\ -\nabla_q V(q,\theta) \\ 0 \end{bmatrix},$$

and

$$F_2 = \begin{bmatrix} M^{-1}p \\ \hat{M}^{-1}\pi \\ 0 \\ -\nabla_\theta V(q,\theta) \end{bmatrix}.$$

A reversible method could be constructed by symmetric composition of the flows on these two vector fields, i.e., by integrating the vector field F_1 for a half timestep, then integrating F_2 for a full timestep, and finally integrating F_1 again for half a timestep. This method would require the following steps. First the "slow momentum variable" p would be pushed forward for a half-step:

$$p^{n+1/2} = p^n - \frac{h}{2}\nabla V(q^n, \theta^n).$$

During the propagation of F_2 observe that p is fixed and q moves along a straight line defined by

$$\bar{q}(t) = q^n + tM^{-1}p^{n+1/2}.$$

At the same time, we must evolve π and θ, the fast variables, according to the differential equations

$$\begin{aligned} \frac{d}{dt}q &= \hat{M}^{-1}\pi, \\ \frac{d}{dt}p &= -\nabla_\theta V(\bar{q}(t), \theta). \end{aligned}$$

Observe that this represents a fast propagation step along a linearly evolving slow dynamic, i.e. the solution of a time-dependent Hamiltonian

$$H_{\text{fast}}(\theta, \pi; \bar{q}) = \frac{1}{2}\pi^T \hat{M}^{-1}\pi + V(\bar{q}(t), \theta).$$

This fast propagation step would typically require implementation of a further numerical integration, and would ultimately result in the computation of θ^{n+1} and π^{n+1}. We can also compute the slow variable position at the end of the timestep:

$$q^{n+1} = q^n + hM^{-1}p^{n+1/2}.$$

Finally, the slow momentum would be updated by the formula

$$p^{n+1} = p^{n+1/2} - \frac{h}{2}\nabla V(q^{n+1}, \theta^{n+1}).$$

This method has several apparent advantages. First, it allows a Störmer-Verlet like integration of the slow variables, but places no restriction on the fast variable propagation. On the other hand, the method exhibits resonant instabilities due to an interaction between the fast dynamics and the long-timestep numerical propagation. Effectively, this can be seen to restrict the usable timestep to a small multiple of the largest timestep which one could expect to use with a standard explicit method such as the Störmer-Verlet method. A great improvement in the properties of the integrator can be obtained by combining the above scheme with an averaging over the fast dynamics during the slow propagation. The reversible averaging method computes a timestep (stepsize h) from time level n to time level $n+1$ as follows:

Algorithm 1. The Reversible Averaging Method.

(1) Propagate the fast variables, then push the slow variables q using a Störmer-Verlet half-step in an averaged slow force:

$$p^{n+1/2} = p^n - \frac{h}{2}\int_0^{h/2} \nabla V(q^n, \theta_n^+(t))dt.$$

Here ${\theta^+}_n(t)$ is obtained by solving the fast Hamiltonian from initial conditions $(\theta, \pi) = (\theta^n, \pi^n)$ with fixed q, i.e. by solving $H_{\text{fast}}(\theta, \pi; q^n)$.

(2) Next, propagate the vector field F_2 for a timestep as in the method discussed previously (i.e. propagating the fast variables under H_{fast} while pushing q along a linear path).

(3) $$p^{n+1} = p^{n+1/2} - \frac{h}{2} \int_{-h/2}^{0} \nabla V(q^n, \theta_{n-1}^-(t))dt,$$

where θ_{n-1}^- is obtained by solving $H_{\text{fast}}(\theta, \pi; q^{n+1})$ *backwards* in time from the step endpoint.

The reversible averaging method has been analyzed in [8] and shown to be resonance-free for a two degree of freedom linear model problem. Numerical experiments were performed on linear and simple nonlinear Hamiltonian systems confirming this property. In the sequel we will attempt to apply this method in a model setting arising in gravitational dynamics.

3 Gravitational Model Problem

Gravitational N-body problems arise in stellar and solar system dynamics. Issues for numerical integration of such problems are discussed in [6,7,12]. As a first step, we consider a heterogeneous N-body problem based on distance potentials only and consisting of isolated bodies and a few spatially localized bound pairs of bodies (binaries). It is to be understood that the techniques developed here are applicable to a much wider class of gravitational problems, but it is conceptually simpler to focus on a sub-class.

The potential energy of the system divides into four terms: (1) the internal potential energies of the binaries, (2) potentials between isolated bodies, (3) potentials between a body and a binary, and (4) potentials between pairs of binaries. Our guiding assumption is that most of the interaction terms between bodies and binaries are relatively weak compared to the binary coupling, so that if all binaries were replaced by singlets, the simulation could be conducted with a substantially larger timestep.

The simplest representative situation is a three-body system modelling a binary in interaction with a singlet. Suppose q_1, q_2 are the positions of the binary pair (corresponding momenta p_1, p_2), and q_3 is the position of the third body, so the kinetic and potential energies can be written

$$T = \frac{1}{2} \sum_{i=1}^{3} m_i \left| \frac{d}{dt} q_i \right|^2, \quad V = \phi_{12}(|r_{12}|^2) + \phi_{13}(|r_{13}|^2) + \phi_{23}(|r_{23}|^2), \tag{6}$$

where $r_{ij} = q_i - q_j$.

We will assume that the masses of the bodies are ordered $m_1 < m_2 < m_3$ and the initial conditions are such that the first and second bodies are bound and orbiting the third body, so that the orbit has the appearance shown at left in Figure 1. (In this diagram, the origin has been fixed at the coordinates of the heavy third body.)

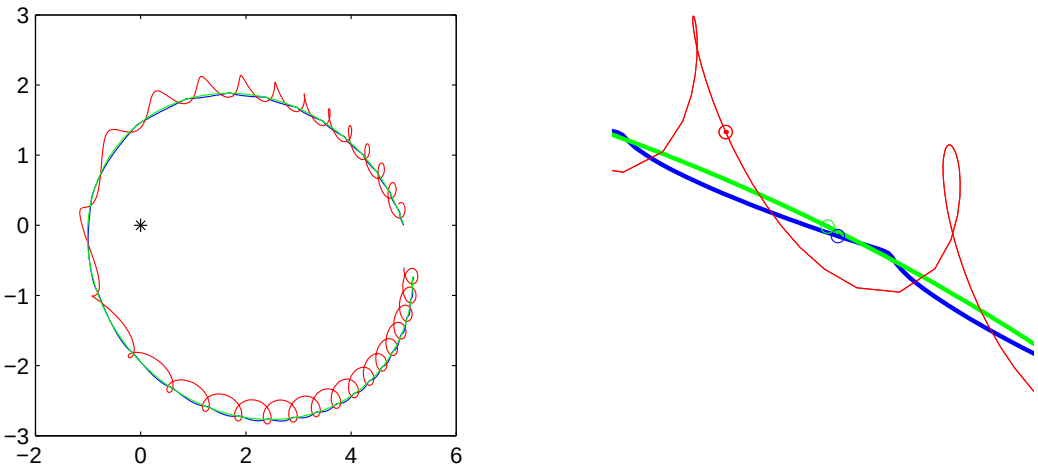

Fig. 1. A sample orbit of a three-body problem (left) with a close up of the dynamics over time (right). The thin curve is the traced orbit of the light body (q_1), the solid heavy curve represents the motion of q_2 and the broken heavy curve is the motion of the centre of mass of the q_1, q_2 subsystem.

Note that the motion of the centre of mass of the q_1, q_2 pair, depicted by the heavy broken line on the right in Figure 1, is slowly varying. It is this variable that would be treated as the slow variable in the reversible averaging method.

4 Internal Coordinates

As we shall see, it is advantageous in the implementation of the algorithm to work in an internal coordinate representation for local groups of bodies. These coordinates provide an elementary separation of scales and also aid the efficient implementation of the reversible averaging method. The expansion of the potential in terms of internal coordinates for the binary and an interaction potential with external bodies is straightforward. The three-body model is adequate to demonstrate this.

We first define (barycentric) coordinates

$$\bar{q} = \frac{m_1 q_1 + m_2 q_2}{M}, \qquad \Delta = q_2 - q_1,$$

where $M = m_1 + m_2$. In these coordinates, the kinetic energy metric remains diagonal,

$$T = \frac{1}{2} M \left| \frac{d}{dt} \bar{q} \right|^2 + \frac{1}{2} \hat{M} \left| \frac{d}{dt} \Delta \right|^2 + \frac{1}{2} m_3 \left| \frac{d}{dt} q_3 \right|^2 ,$$

with $\hat{M}$ the *reduced mass* ($\hat{M} = (1/m_1 + 1/m_2)^{-1}$), and the potential energy is now

$$V = \phi_{12}(|\Delta|^2) + \phi_{13}(|\bar{q} - q_3 - \frac{m_2}{M}\Delta|^2) + \phi_{23}(|\bar{q} - q_3 + \frac{m_1}{M}\Delta|^2).$$

Taylor series expansion leads to the following expression:

$$V = \phi_{12}(|\Delta|^2) + \Phi^{(0)}(\bar{q} - q_3) + \Phi^{(1)}(\bar{q} - q_3) \cdot \Delta + \Delta^T \Phi^{(2)}(\bar{q} - q_3)\Delta + \ldots , \qquad (7)$$

where $\Phi^{(0)}$ is scalar valued, $\Phi^{(1)} : \mathbf{R}^3 \to \mathbf{R}^3$, $\Phi^{(2)} : \mathbf{R}^3 \to \mathbf{R}^{3\times 3}$, and so on. These first few functions are (with $r = \bar{q} - q_3$)

$$\Phi^{(0)}(r) = \phi_{13}(|r|^2) + \phi_{23}(|r|^2),$$

$$\Phi^{(1)}(r) = -2 \left[\frac{m_2}{M} \phi'_{13}(|r|^2) - \frac{m_1}{M} \phi'_{23}(|r|^2) \right],$$

and

$$\Phi^{(2)}(r) = \left[\left(\frac{m_2}{M}\right)^2 \phi'_{13}(|r|^2) + \left(\frac{m_1}{M}\right)^2 \phi'_{23}(|r|^2) \right] I + 2 \left[\left(\frac{m_2}{M}\right)^2 \phi''_{13}(|r|^2) + \left(\frac{m_1}{M}\right)^2 \phi''_{23}(|r|^2) \right] r r^T .$$

We now specialize to the case of gravitation,

$$\phi_{ij} = \frac{-G m_i m_j}{|q_i - q_j|},$$

for which the formulas in the expansion simplify considerably. In particular, we find that the odd order terms (in powers of Δ) vanish:

$$\Phi^{(0)}(r) = -\frac{GMm_3}{|r|},$$

$$\Phi^{(1)}(r) = 0,$$

and

$$\Phi^{(2)}(r) = \frac{G\hat{M}m_3}{2}|r|^{-3}(I - 3\frac{rr^T}{|r|^2}).$$

We see that the terms of the potential series can be expected to fall off extremely rapidly in this case, since the successive terms involve not only increasing (even) powers of Δ, but also *odd reciprocal powers of the interbody separation* r. Moreover, it would not be terribly difficult or costly to include additional terms in the series of orders $O(|\Delta|^4|r|^{-5})$ and beyond if accuracy were found to be compromised by truncation to terms of second order in Δ.

Extending the force expansion to the case of a single binary in interaction with many distant singletons is straightforward. We simply add terms of the same form for each distant pair, thus for a collection of N bodies, the first two of which are bound, we obtain an expansion of the same form as (7), but with

$$\Phi^{(0)} = -\sum_{j=3}^{N} \frac{GMm_j}{|r_j|},$$

$$\Phi^{(1)} = 0,$$

and

$$\Phi^{(2)} = \sum_{j=3}^{N} \frac{G\hat{M}m_3}{2}|r_j|^{-3}(I - 3\frac{r_j r_j^T}{|r_j|^2}),$$

where $r_j = \bar{q} = q_j$.

4.1 Binary-binary interaction

When the system consists of two binaries in interaction, the potential series becomes slightly more complicated, but, in the case of gravitation, the same observations hold regarding the fall-off of terms. Let m_i, $i = 1, \ldots 4$, represent the masses of the four bodies, q_i and p_i the position and momemtum vector, respectively, of the ith body, and define

$$M_1 = m_1 + m_2, \quad \hat{M}_1 = (1/m_1 + 1/m_2)^{-1},$$

$$M_2 = m_3 + m_4, \quad \hat{M}_2 = (1/m_3 + 1/m_4)^{-1}.$$

Define further

$$\bar{q}_1 = \frac{m_1 q_1 + m_2 q_2}{M_1}, \quad \Delta_1 = q_2 - q_1, \quad \bar{q}_2 = \frac{m_3 q_3 + m_4 q_4}{M_2}, \quad \Delta_2 = q_4 - q_3.$$

With $r = \bar{q}_1 - \bar{q}_2$, we next set

$$\begin{aligned}
\Delta_{13} &= -\frac{m_2}{M_1} r \cdot \Delta_1 + \frac{m_4}{M_2} r \cdot \Delta_2, \\
\Delta_{14} &= -\frac{m_2}{M_1} r \cdot \Delta_1 - \frac{m_3}{M_2} r \cdot \Delta_2, \\
\Delta_{23} &= \frac{m_2}{M_1} r \cdot \Delta_1 + \frac{m_4}{M_2} r \cdot \Delta_2, \\
\Delta_{24} &= \frac{m_2}{M_1} r \cdot \Delta_1 - \frac{m_3}{M_2} r \cdot \Delta_2.
\end{aligned}$$

The kinetic energy in the internal coordinates is

$$T = \frac{1}{2} M_1 |\frac{d}{dt} \bar{q}_1|^2 + \frac{1}{2} \hat{M}_1 |\frac{d}{dt} \Delta_1|^2 + \frac{1}{2} M_2 |\frac{d}{dt} \bar{q}_2|^2 + \frac{1}{2} \hat{M}_2 |\frac{d}{dt} \Delta_2|^2,$$

and a little work shows that the potential expansion can be written, to terms of second order, in the form (the superscript indicates the order of truncation of the series expansion):

$$\begin{aligned}
V^{(2)} = &\phi_{12}(|\Delta_1|^2) + \phi_{34}(|\Delta_2|^2) \\
&+ \sum_{\alpha,\beta} \phi_{\alpha\beta}(|r|^2) \\
&+ 2 \sum_{\alpha,\beta} \phi'_{\alpha\beta}(|r|^2) \Delta_{\alpha\beta} \\
&+ \sum_{\alpha,\beta} (\phi'_{\alpha\beta}(|r|^2) |\Delta_{\alpha\beta}|^2 I + 2\phi''_{\alpha\beta}(|r|^2) |r \cdot \Delta_{\alpha\beta}|^2,
\end{aligned}$$

where the sums extend over pairs α, β with $\alpha \in \{1, 2\}$ and $\beta \in \{3, 4\}$.

In the case of gravitation, many terms again fall out, and we arrive at (still to second order in Δ_1 and Δ_2)

$$\begin{aligned}
V^{(2)} = &-\frac{G M_1 M_2}{|r|} - \frac{G m_1 m_2}{|\Delta_1|} - \frac{G m_3 m_4}{|\Delta_2|} \\
&+ G \hat{M}_1 M_2 |r|^{-3} \Delta_1^T (I - 3\frac{r r^T}{|r|^2}) \Delta_1 + G M_1 \hat{M}_2 |r|^{-3} \Delta_2^T (I - 3\frac{r r^T}{|r|^2}) \Delta_2. \quad (8)
\end{aligned}$$

Note the extraordinary elimination of cross terms (involving products of Δ_i and Δ_j) in this expression, something which only happens due to the special nature of the gravitational potential. In the general case, the bodies will divide into isolated particles and close pairs, and the potential energy can be decomposed into a sum of terms of the forms (7) and (8). As many terms as needed may be maintained in this series. In the case of a system of gravitating binaries and isolated bodies, we may use a unified notation, writing

$$V^{(2)} = -\sum_{i<j} \frac{GM_iM_j}{|r_{ij}|} + \sum_{i\in B}\sum_{j\neq i} G\hat{M}_iM_j|r_{ij}|^{-3}\Delta_i^T(I - 3\frac{r_{ij}r_{ij}^T}{|r_{ij}|^2})\Delta_i, \tag{9}$$

where B is a set of indices of the binaries, M_i is either the mass of an isolated body or the average of masses of the corresponding binary pair, and $\hat{M}_i$ is the reduced mass of the ith binary.

5 Resolution of binaries: averaging and propagation

The reversible averaging algorithm (Algorithm 1) requires accurate integration of the binaries, both for averaging and during propagation. The averaging in steps 1 and 3 is performed with respect to the dynamics of the binaries in a fixed field of distant bodies. Here we examine the cost of performing these steps and show that these can be implemented in an efficient way.

Following coordinate transformation, the Hamiltonian is written in terms of the (supposed slowly varying) positions of isolated bodies and centers of mass of the binaries together with the fast rotating separation vectors for each pair. As we have seen, the potential can be written in the form of a series of terms in Δ_i with coefficient functions of the slowly varying vectors r_{ij}. In the original reversible averaging method, these slowly varying vectors would be evolved along a linear path $\hat{r}_{ij}(t)$, so the force would need to be computed at each step of the fast evolution. This approach would eliminate any advantage that we might hope to achieve from the separation of scales. To illustrate, suppose that $\bar{r}_{ij}$, $1 \leq i < j < N$ represent the separation vectors of a system of N binaries. The fast component for the ith binary evolves in the truncated potential series

$$V_i^{(2)} = -\frac{\gamma}{|\Delta_i|} + \Delta_i^T\Phi_i^{(2)}\Delta_i,$$

with

$$\Phi_i^{(2)} = \sum_{j \neq i} G\hat{M}_i M_j |\bar{r}_{ij}|^{-3} (I - 3\frac{\bar{r}_{ij}\bar{r}_{ij}^T}{|\bar{r}_{ij}|^2}).$$

During the first and third steps of Algorithm 1, $\Phi^{(2)}$ would simply be held fixed and the resulting system for Δ_i then solved in a time-reversible way. Thus the i 3×3 matrices $\Phi_i^{(2)}$ are computed in a total of $O(N^2)$ floating operations, but this need only be done at the beginning (and end) of the slow timestep. Since the quadratic term can be assumed to be relatively weak compared to the Coulombic term, it is natural to use a simple Trotter factorization for this stage, consisting of a half $\Delta\tau$ step in the quadratic term, followed by a timestep with the fast kinetic energy + Coulombic potential, then another half–step with the quadratic term. Of course the Coulombic term yields a pure Kepler problem. We suggest solving this part using some sort of fast Kepler solver, for example the method of [16] which is a second order, energy-preserving symplectic-reversible discretization based on the Kustaanheimo-Stiefel linearizing variables, a scheme which avoids transcendental function evaluations.

During the fast propagation stage in the middle of the timestep, the slow separation variables $\bar{r}_{ij}$ would normally be evolved along linear paths, leading to a much more costly $O(KN^2)$ calculation at each long timestep, where K is the number of fast timesteps per long step. Here we propose instead the following modification: *interpolate the potential energy (and force) instead of the slow variable.* This is equivalent to averaging each coefficient in the Δ Taylor expansion; in this way, the second order accuracy is preserved, but the calculation of the forces can be done with computational complexity essentially independent of K.

Define

$$\Phi_i^{(2)}[\tau] = (1 - \tau/\Delta t)\Phi_i^{(2)}(\{\bar{r}_{ij}^0\}) + (\tau/\Delta t)\Phi_i^{(2)}(\{\bar{r}_{ij}^1\}).$$

The propagation algorithm is now almost identical to that of the forward and backward averaging stages, except that in the first half step of the Trotter factorization, the force term is

$$-\Phi_i^{(2)}[k\tau]\Delta_i,$$

while in the third stage, we use

$$-\Phi_i^{(2)}[(k+1)\tau]\Delta_i.$$

These force evaluations are essentially 'free, ' in that they involve very little additional

work at each step, compared to the other costs involved (for example, no new square roots, other than those for the binary separations would need to be calculated at the intermediate steps). Note that this modification of the reversible averaging does not effect the stability analysis (or lack of resonance) since the modification only constitutes a change in the case of nonlinear models.

5.1 Cost of the Force Averaging

For propagation of the slow variables, we must also compute the averaged force acting on the slow variables due to the effects of distant bodies and binaries along the fast averaging trajectories; the challenge is to do this efficiently. The force term for the ith center of mass takes the form

$$\begin{aligned} F_i = &-\sum_{j\neq i} G\hat{M}_i M_j [15|\bar{r}_{ij}|^{-7}(\bar{r}_{ij}\cdot\Delta_i)^2\bar{r}_{ij} - 6|\bar{r}_{ij}|^{-5}(\bar{r}_{ij}\cdot\Delta_i)\Delta_i] \\ &-\sum_{j\neq i} GM_i\hat{M}_j [15|\bar{r}_{ij}|^{-7}(\bar{r}_{ij}\cdot\Delta_j)^2\bar{r}_{ij} - 6|\bar{r}_{ij}|^{-5}(\bar{r}_{ij}\cdot\Delta_j)\Delta_j] \end{aligned}$$

with fixed slow variables $\{r_{ij}\}$. At first glance, it looks as though an $O(N^2)$ force calculation is needed for each *fast* step, resulting in an expensive $O(N^2K)$ scheme, but this computation can be made much more efficient by careful rearrangements as we now show.

Let $\bar{q}_i = (\bar{x}_i, \bar{y}_i, \bar{z}_i)^T$ be the coordinates of the ith center of mass, and denote by $F_{\bar{x}_i}, F_{\bar{y}_i}, F_{\bar{z}_i}$ the force acting on the corresponding coordinates. Finally let $\Delta_i^{(k)} = (\Delta_{x_i}^{(k)}, \Delta_{y_i}^{(k)}, \Delta_{z_i}^{(k)})^T$ represent the fast variable at the kth fast step. The average for the first component of the force then takes the form

$$\begin{aligned} \frac{1}{K}\sum_{k=1}^{K} F_{x_i} = -\frac{1}{K}\sum_{k=1}^{K}\sum_{j\neq i} G\hat{M}_i M_j \Big(&15|\bar{r}_{ij}|^{-7}(\bar{r}_{ij}\cdot\Delta_i^{(k)})^2(x_i - x_j) - \\ &6|\bar{r}_{ij}|^{-5}(\bar{r}_{ij}\cdot\Delta_i^{(k)})\Delta_{x_i}^{(k)}\Big) \\ +GM_i\hat{M}_j \Big(&15|\bar{r}_{ij}|^{-7}(\bar{r}_{ij}\cdot\Delta_j^{(k)})^2(x_i - x_j) - 6|\bar{r}_{ij}|^{-5}(\bar{r}_{ij}\cdot\Delta_j^{(k)})\Delta_{x_j}^{(k)}\Big) \end{aligned}$$

Let us consider each of the four terms of the summand separately. The first term can be written as

$$-15G\frac{1}{K}\sum_{k=1}^{K}\sum_{j\neq i}\hat{M}_i M_j|\bar{r}_{ij}|^{-7}(\bar{r}_{ij}\cdot\Delta_i^{(k)})^2(x_i - x_j)$$

$$= -15G\frac{1}{K}\sum_{k=1}^{K}\sum_{j\neq i}\hat{M}_i M_j(x_i - x_j)|\bar{r}_{ij}|^{-7}[\Delta_i^{(k)}]^T\bar{r}_{ij}\bar{r}_{ij}^T\Delta_i^{(k)}$$
$$= -15G\frac{1}{K}\sum_{k=1}^{K}[\Delta_i^k]^T A_{ij}\Delta_i^k,$$

where

$$A_{ij} = \sum_{j\neq i}\hat{M}_i M_j(x_i - x_j)|\bar{r}_{ij}|^{-7}\bar{r}_{ij}\bar{r}_{ij}^T$$

is a 3×3 matrix that need only be computed once per long timestep. The computational cost of this part of the calculation, including the terms for each i, is $O(N^2 + NK)$.

For the second term, we have

$$6G\frac{1}{K}\sum_{k=1}^{K}\sum_{j\neq i}\hat{M}_i M_j|\bar{r}_{ij}|^{-5}(\bar{r}_{ij}\cdot\Delta_i^{(k)})\Delta_{x_i}^{(k)}$$
$$= 6G\frac{1}{K}\sum_{k=1}^{K}(\alpha_i(\Delta_{x_i}^{(k)})^2 + \beta_i\Delta_{x_i}^{(k)}\Delta_{y_i}^{(k)} + \gamma_i\Delta_{x_i}^{(k)}\Delta_{z_i}^{(k)}),$$

where

$$\alpha_i = \sum_{j\neq i}\hat{M}_i M_j|\bar{r}_{ij}|^{-5}(\bar{x}_i - \bar{x}_j),$$
$$\beta_i = \sum_{j\neq i}\hat{M}_i M_j|\bar{r}_{ij}|^{-5}(\bar{y}_i - \bar{y}_j),$$
$$\gamma_i = \sum_{j\neq i}\hat{M}_i M_j|\bar{r}_{ij}|^{-5}(\bar{z}_i - \bar{z}_j).$$

each such coefficient must be computed only once per timestep, and the complexity is again only $O(N^2 + NK)$. The last two components embody the sum of the effects of the distant binaries on the center of mass of the ith. Here we use the alternate arrangement of the terms of the summation:

$$-15G\frac{1}{K}\sum_{k=1}^{K}\sum_{j\neq i}\hat{M}_i M_j|\bar{r}_{ij}|^{-7}(\bar{r}_{ij}\cdot\Delta_j^{(k)})^2(x_i - x_j)$$
$$= -15G\sum_{j\neq i}\hat{M}_i M_j(x_i - x_j)|\bar{r}_{ij}|^{-7}\frac{1}{K}\sum_{k=1}^{K}\bar{r}_{ij}^T\Delta_i^{(k)}[\Delta_i^{(k)}]^T\bar{r}_{ij}^T$$

$$= -15G \sum_{j \neq i} \hat{M}_i M_j (x_i - x_j) |\bar{r}_{ij}|^{-7} \bar{r}_{ij}^T B_i \bar{r}_{ij}^T,$$

where

$$B_i = \frac{1}{K} \sum_{k=1}^{K} \Delta_i^{(k)} [\Delta_i^{(k)}]^T.$$

Since we must compute N such B_i each requiring $O(K)$ work, then, with these computed, the force calculation requires another $O(N^2)$ steps to produce the result. A similar story holds for the fourth term.

Thus we have succeeded in reducing the computational effort to $O(N^2 + NK)$; for large N and a number of fast timesteps K substantially smaller than N, the work for the reversible averaging method will be only a little larger than that of a step of a standard numerical method.

6 Numerical Experiment: a Three-Body Problem

Next, we describe the application of the method to a 3-body model problem. Our purpose is to investigate the large timestep observed stability behavior of the method in a gravitational application. In our experiments, we did not test the use of truncated force expansions, but only the potential effectiveness of the reversible averaging scheme for the 3-body model, using the barycentric separating coordinates described in the text.

In each experiment, we integrated the system (6) with the heavy body fixed to the origin using the same set of initial conditions, producing in each case approximations to the orbit shown in Figure 1. In this simulation, the binary pair approaches the origin, where the orbit is progressively disturbed by the heavy body. The standard leapfrog-Störmer-Verlet integrator became unstable at a stepsize of approximately $h = 0.008$. We implemented the reversible multiple time-scale integrator, using the variable decomposition described in the previous pages.

Our initial observation was that the stepsize could be improved beyond the leapfrog threshold, but only modestly. A representative simulation is illustrated in Figure 2. Here the left hand diagram shows the planar positions of the bodies with the time variable along the z-axis. The right figure shows the fluctuations in the energy vs. time.

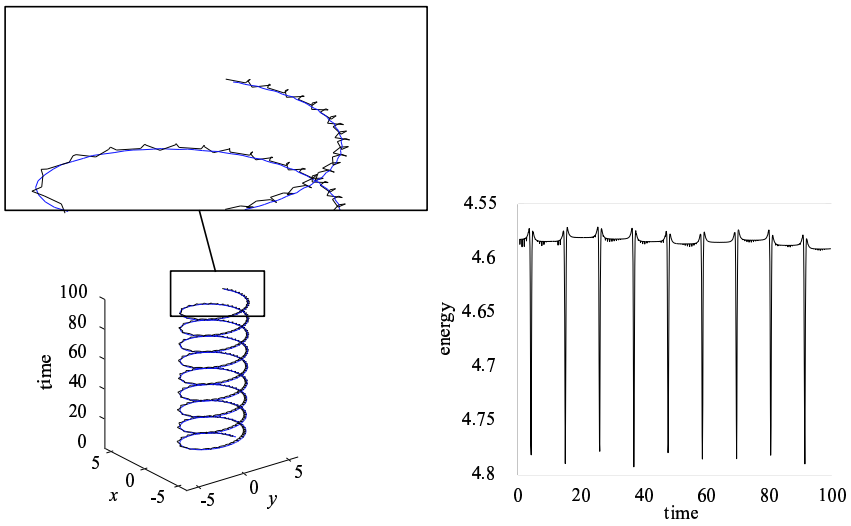

Fig. 2. Integration of the 3-body model problem using reversible averaging. Left: a graph of the planar positions of the particles with the time variable running along the z-axis with inset showing a close up view. Right: the energy error vs. time showing the large spikes and energy drift caused by close approaches of the two bodies to the fixed body at the origin.

Upon closer examination it was found that accuracy was impaired near the approach of the binary to the origin. We can see the effect of such approaches in the right hand side of Figure 2. The problem is that when using standard (fixed stepsize) leapfrog, the slow dynamics of the centre of mass become unstable at a stepsize only slightly above the stepsize needed to resolve the oscillators: in our terminology, this problem would not have a strong separation between timescales.

The key to going further is to note that the Keplerian centre of mass dynamics requires the use of a variable stepsize. We should rather compare variable stepsize integration with and without the multiple scale decomposition. The natural way to implement variable stepsize in this setting is based on a reversible variable stepsize strategy [19]. Such methods and their implementation, analysis, extension to higher order, etc., are treated in [19,18,15]. We do not discuss these methods here in detail, but merely point out that, following [18], if Φ_h is an arbitrary reversible fixed stepsize integrator, then the mapping from (z^n, h_n) to (z^{n+1}, h_{n+1}) defined by

$$\begin{aligned} z^{n+1/2} &= \Phi_{h_n/2}(z^{n+1/2}) \\ h_{n+1}^{-1} + h_n^{-1} &= [g(z^{n+1/2})\Delta\tau]^{-1} \\ z^{n+1} &= \Phi_{h_{n+1}/2}(z^{n+1/2}) \end{aligned}$$

is a time-reversible variable stepsize method. For our example, we used a time transformation g of the form

$$g(z) = r^{3/2}$$

where r is the distance between the centre of mass of the binary pair and the origin.

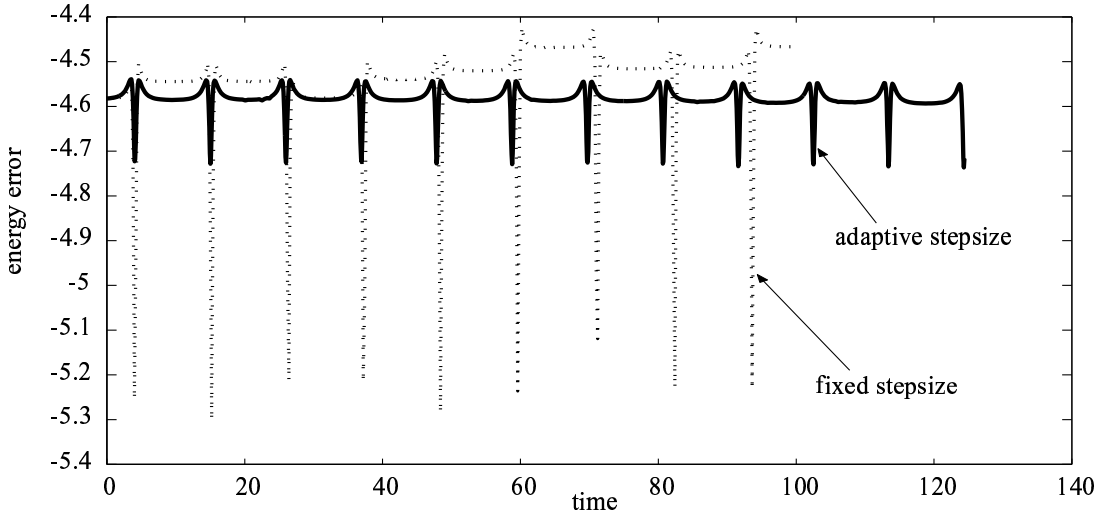

Fig. 3. Reversible averaging combined with time-reversible variable stepsizes (adaptive reversible averaging) improves the integration through approach to the origin and the drift in energy. (In the fixed stepsize run (dash-dot) the long stepsize was 0.2; in the variable stepsize calculation (solid), the same total number of long timesteps was used as in the fixed stepsize calculation.)

With the reversible variable stepsize method, the results obtained are greatly improved. We found that it was possible to carry out integrations stably with an average stepsize as much as 50 times the fixed stepsize leapfrog stability threshold. A typical comparison is shown in Figure 3. More importantly, there is no evidence of resonance in an extensive search. This is illustrated in Figure 4 which shows the energy error to timestep relationship. 1000 simulations on a fixed time interval $[0, 100]$ were performed to create this figure. As the long stepsize is increased, the number of fast timesteps is increased proportionately, so that the same (inner) fast timestep is used in each run.

The 3-body model problem possesses an adiabatically separated fast energy when the separation of the $q_1 q_2$ subsystem is sufficiently large. This adiabatic separation breaks down in close approach, during which an exchange of energy takes place between the Keplerian dynamics of the centre of mass of the binary and the dynamics of the binary itself. In order to understand better the accuracy of the adaptive reversible averaging algorithm, we looked at how accurately these transitions were computed by the scheme. In Figures 5-7, the effect of the close approach on the adiabatic fast energy (the Keplerian energy of the binary)is followed for three average long stepsizes

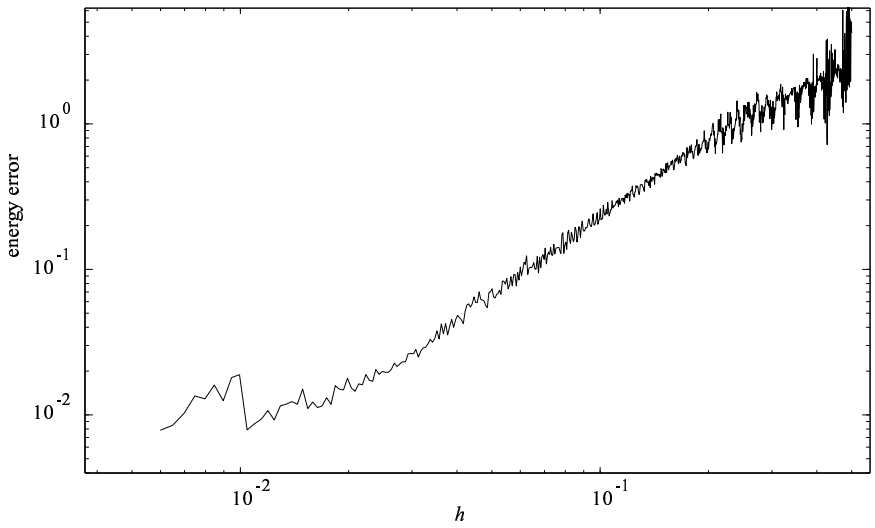

Fig. 4. A timestep-error diagram for the adaptive reversible averaging algorithm shows no sign of resonant instability in 1000 runs over a range of long stepsizes up to 50 times the fixed stepsize leapfrog stability threshold.

($\bar{h} = 0.08$, $\bar{h} = 0.4$ and $\bar{h} = 0.8$), and compared against a relatively accurate leapfrog-computed trajectory.

Observe that at $\bar{h} = 0.08$ (four fast steps per long timestep), some accuracy is lost during the transition itself, but—importantly—the correct fluctuation is recovered in the fast energy. A similar situation is observed until $\bar{h} = 0.4$ (50 fast steps per long timestep). Only at $\bar{h} = 0.8$ (long timestep 100 times the Adaptive Verlet stability threshold) do we see a serious breakdown of the energetic transition.

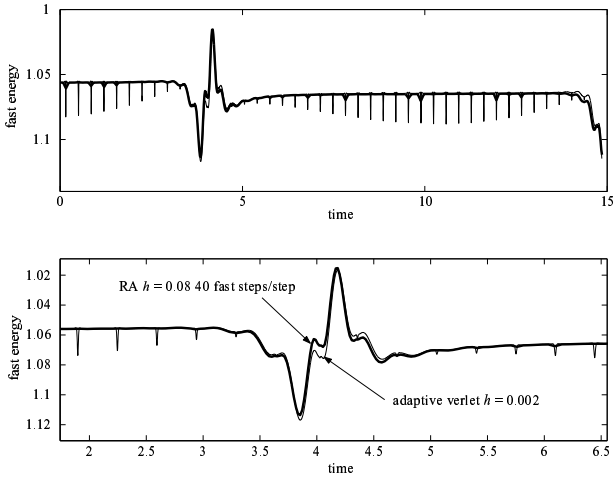

Fig. 5. Effect of the close approach on the adiabatic fast energy, comparing the adaptive reversible averaging ($\bar{h} = 0.08$) and leapfrog ($h = 0.002$) integrators .

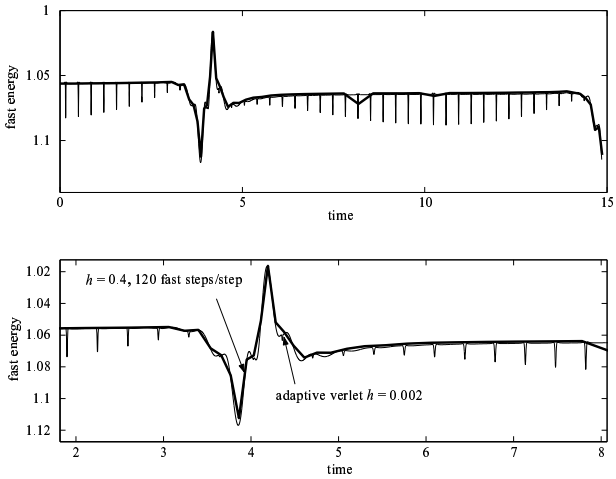

Fig. 6. Effect of the close approach on the adiabatic fast energy, comparing the adaptive reversible averaging ($\bar{h} = 0.4$) and leapfrog ($h = 0.002$) integrators .

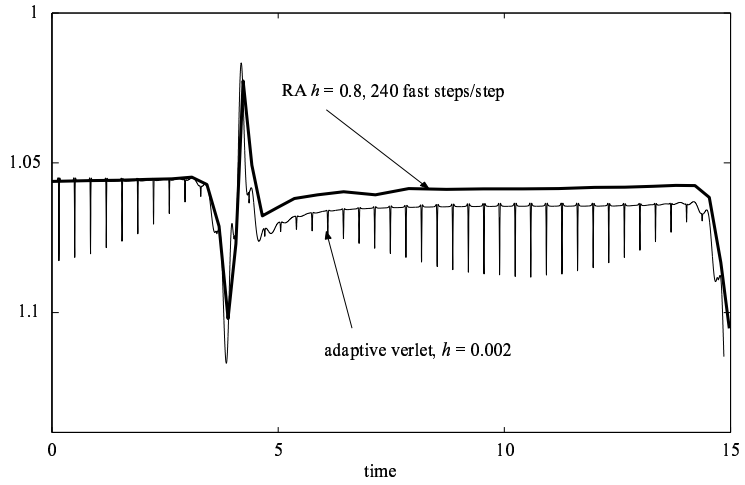

Fig. 7. Effect of the close approach on the adiabatic fast energy, comparing the adaptive reversible averaging ($\bar{h} = 0.8$) and leapfrog ($h = 0.002$) integrators.

7 Conclusion

The theory and experiments given here offer convincing evidence for the potential of the combined reversible averaging/reversible variable stepsize method for gravitational N-body simulations, but much more remains to be done. More careful treatment of the tidal effects (through the use of perturbation series) would likely be needed

in solar system dynamics; this issue needs to be examined in detail, and for realistic applications. An implementation that incorporates a better Kepler solver in the fast propagator would be valuable in many applications. The switching idea of [17] might be valuable for switching fast variables or for adapting the number of terms retained in the perturbation series of the potential.

References

[1] Murray, N. and Holman, M.J., The role of chaotic resonances in the Solar System, *Nature* **410**, 773-779 (2001).

[2] Lecar, M., Franklin, F.A., Holman, M.J., Murray, N.J., Chaos in the Solar System, *Annual Review of Astronomy and Astrophysics* **39**, 581-631 (2001).

[3] Holman, M.J. and Wiegert, P., Long-term stability of planets in binary systems , *Astron. J.* **117**, 621-628. (1999)

[4] Preto, M., and Tremaine, S., A class of symplectic integrators with adaptive timestep for separable Hamiltonian systems, *Astron. J* **118**, 2532 (1999).

[5] Wiegert, P., and Tremaine, S., The evolution of long-period comets, *Icarus* **137**, 84 (1999).

[6] Aarseth, S.J., Direct methods for N-body simulation, in *Multiple Time Scales*, Eds J. U. Brackbill and B.I. Cohen, Academic Press, NY, 1985.

[7] Heggie, D.C., The N-body problem in stellar dynamics, in *Long-Term Dynamical Behavior of Natural and Artificial N-Body Systems*, Ed. A.E. Roy, NATO ASI Series, Kluwer, Dordnecht, 1988.

[8] Leimkuhler, B. and Reich, S., A reversible averaging integrator for multiple time-scale dynamics. J. Comput. Physics **171** , 95-114, 2001

[9] Gear, C.W., and Wells, D.R., Multirate linear multistep methods, *BIT*, **24**, 484-502, 1984.

[10] Grobmuller, H., Heller, H., Windemuth, A., and Schulten, K., Generalized Verlet algorithm for efficient molecular dynamics simulations with long-range interactions, *Molecular Simulation* **6**, 121-142, 1991.

[11] Tuckerman, M., Berne, B., J., and Martyna, G.J., Reversible multiple time-scale molecular dynamics, *J. Chem. Phys.*, **97**, 1990-2001, 1992.

[12] Wisdom, J. and Holman, M., Symplectic maps for the N-body problem, *The Astronomical Journal* **102**, 1528, 1991.

[13] Garcia–Archilla, B., Sanz-Serna, J.M., and Skeel, R.D., Long time-step methods for oscillatory differential equations, *SIAM J. Sci. Comput.* **20**, 930-963, 1998.

[14] Izaguirre, J., Reich, S., and Skeel, R.D., Longer time steps for molecular dynamics, *J. Chem. Phys.*, **110**, 9853–9864, 1999.

[15] Calvo, M.P. and Hairer, E., Accurate long-term integration of dynamical systems, Applied Numerical Mathematics **18**, 95-105, 1995.

[16] Leimkuhler, B., Reversible adaptive regularization: perturbed Kepler motion and classical atomic trajectories, *R. Soc. Lond. Philos. Trans., Ser. A: Math., Phys., Eng. Sci.* **357**, 1101-1133, 1999.

[17] Kværnø, A., and Leimkuhler, B., A time-reversible, regularized, switching integrator for the N-body problem, *SIAM J. Sci. Comput.* **22**, 1016-1035, 2001.

[18] Holder, T., Leimkuhler, B., and Reich, S., Explicit variable stepsize and time-reversible integration, *Applied Numerical Mathematics* **39**, 367-377, 2001.

[19] Huang, W., and Leimkuhler, B., The Adaptive Verlet Method, *SIAM J. Sci. Comput.* **18**, 239, 1997.

[20] Cirilli, S., Hairer, E., and Leimkuhler, B., Asymptotic error analysis of the Adaptive Verlet method, *BIT* **39**, 25-33, 1999.